Article ID: 1003-6326(2003)05-1108-04

Friction stir welding characteristics of two aluminum alloys①

LIU Hui-jie(刘会杰)[1,2], FUJII Hidetoshi(藤井英俊)[1],
MAEDA Masakatsu(前田将克)[1], NOGI Kiyoshi(野城清)[1]
(1. Joining and Welding Research Institute, Osaka University, Osaka 567-0047, Japan;
2. State Key Laboratory of Advanced Welding Production Technology,
Harbin Institute of Technology, Harbin 150001, China)

Abstract: The friction stir welding characteristics of the strain-hardened AA1050-H24 and precipitate-hardened AA2017-T351 aluminum alloys were examined in order to reveal the effects of the alloy properties on the friction stir welding behavior of the base materials. The results show that (1) for AA1050-H24, the weld possesses a smooth surface and clear ripples, there is no elliptical weld nugget in the weld, there is not discernible interface between the stir zone and the thermo-mechanically affected zone(TMAZ), and the internal defect of the weld looks like a long crack and is located in the lower part of the weld; (2) for AA2017-T351, the weld usually possesses a rough surface and visible ripples, the elliptical weld nugget clearly exists in the weld and there is obvious plastic flow and a discernible interface between the nugget and the TMAZ, and the internal defect of the weld is composed of many voids and distributed in the middle part of the weld; (3) the effective ranges of the welding parameters for AA1050-H24 and AA2017-T351 are both narrow, especially for the latter; and (4) the tensile strength efficiencies of the joints for the two typical alloys are similar, i e 79% for AA1050-H24 and 82% for AA2017-T351.

Key words: friction stir welding; aluminum alloy; welding parameter; welding defect; tensile strength
CLC number: TG 453.9 **Document code:** A

1 INTRODUCTION

Friction stir welding(FSW) is a promising welding process that can produce high-quality and low-cost joints[1,2]. Especially, it can eliminate some welding defects such as cracking and porosity often associated with fusion welding processes[2,3], and thus is suited to weld heat-treatable aluminum alloys that are difficult to fusion weld[4,5]. Recent studies on the microstructural characteristics and mechanical properties of the friction stir welded joints have indicated that different aluminum alloys have different FSW characteristics[6-17]. With respect to the mechanical properties of the weld joints, the heat-treatable aluminum alloys such as 2014-T651[6], 2024-T3/T351/T6[7-10], 2195-T8[11], 7075-T651[12] and 7475-T76[13] alloys undergo a process of dissolution or growth of the strengthening precipitates during the thermal cycle of FSW, thus resulting in a degradation of the mechanical properties. The strain-hardened aluminum alloys such as 5754[14], 1100[15] and 1050 alloy[16,17] are also softened by FSW because the dislocation density in the weld and heat-affected zone has decreased after welding.

However, the difference in the friction stir welding characteristics among the different aluminum alloys has not been systematically studied or reported, and studying this topic is quite important for us to deeply understand the effects of the alloy properties on the FSW behavior. Therefore, two typical aluminum alloys, strain-hardened AA1050-H24 and precipitate-hardened AA2017-T351, are selected as the experimental materials for the study of the FSW characteristics in this paper. The emphasis is focused on the morphologies and defects of the welds, the mechanical properties of the joints and the affected range of the welding parameters.

2 EXPERIMENTAL

The base materials were 5-mm-thick AA1050-H24 and AA2017-T351 aluminum alloy plates with the chemical compositions and mechanical properties listed in Table 1. The plates were all cut and machined into rectangular welding samples with dimension of 300 mm × 80 mm and they were longitudinally butt-welded using an FSW machine. The welding tool size and welding parameters are listed in Table 2. It should be pointed out that "revolutionary pitch" is a derived welding parameter and is defined as the welding speed divided by the rotating speed. Its physical meaning corresponds to the heat input to a joint.

After welding, the superficial morphologies of the welds were first photographed using a digital camera, and then the joints were cross-sectioned

① **Received date:** 2003-03-13; **Accepted date:** 2003-05-13
Correspondence: LIU Hui-jie, Professor; Tel/Fax: +81-6-68798663; E-mail: lhj@jwri.osaka-u.ac.jp or liuhj@hope.hit.edu.cn

Table 1 Chemical compositions and mechanical properties of base materials

Alloy	Chemical composition/ %									Mechanical property		
	Si	Fe	Cu	Mg	Mn	Ti	Zn	Cr	Al	σ_b/ MPa	σ_s/ MPa	δ/ %
AA1050-H24	0.04	0.32	0.02	0.01	0.00	0.02	0.00	0.00	Bal.	106	68	18.6
AA2017-T351	0.52	0.29	4.29	0.60	0.58	0.02	0.08	0.02	Bal.	428	319	23.8

Table 2 Welding tool size and welding parameters

Alloy	Tool size			Welding parameters			
	Shoulder diameter/ mm	Pin diameter/ mm	Pin length / mm	Tool tilt/ (°)	Rotating speed/ ($r\cdot min^{-1}$)	Welding speed/ ($mm\cdot min^{-1}$)	Revolutionary pitch/ ($mm\cdot r^{-1}$)
AA1050-H24	15	6	4.7	3	1 500	100 - 800	0.07 - 0.53
AA2017-T351	15	6	4.7	3	1 500	25 - 800	0.02 - 0.53

perpendicular to the welding direction for the metallographic analyses and tensile tests using an electrical-discharge cutting machine. The cross-sections of the metallographic specimens were po-lished with an alumina suspension, etched with Keller's reagent (150 mL water, 3 mL nitric acid, 6 mL hydrochloric acid and 6 mL hydrofluoric acid) and observed by optical microscopy. The internal defects of the welds were identified by a metallographic examination, and the effective range of the welding parameters was assessed by the internal defect examination.

The configuration and size of the transverse tensile specimens were referenced to ISO 6892, and the marked length and width of each specimen were 50 mm and 12.5 mm, respectively. Prior to the tensile tests, the Vickers hardness profiles across the stir zone, thermo-mechanically affected zone (TMAZ), heat affected zone (HAZ) and partial base material were measured along the centerlines of the cross-sections of the tensile specimens under a load of 0.98 N for 10 s using an automatic micro-hardness tester. The tensile tests were carried out at room temperature and a crosshead speed of 1 mm/ min using a computer-controlled testing machine, and the tensile properties of each joint were evaluated using three tensile specimens cut from the same joint.

3 RESULTS AND DISCUSSION

3.1 Morphologies and defects of welds

3.1.1 Superficial morphologies of welds

Fig. 1 shows the superficial morphologies of the AA1050-H24 and AA2017-T351 welds performed at the same revolutionary pitch of 0.27 $mm\cdot r^{-1}$. The surface of the AA1050-H24 weld is smoother and the surface ripples are clearer (Fig. 1(a)), while the surface of the AA2017-T351 weld is rougher and the surface ripples are less visible. Also, some oxide scales exist on the surface (Fig. 1(b)). This result indicates that the surface quality of the AA1050-H24 weld is better.

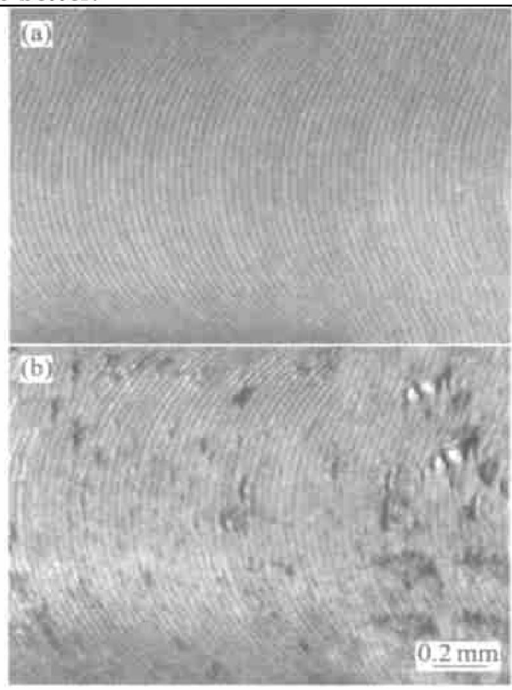

Fig. 1 Superficial morphologies of AA1050-H24(a) and AA2017-T351welds(b)

3.1.2 Internal morphologies of welds

The internal morphologies of the defect-free AA1050-H24 and AA2017-T351 welds are shown in Fig. 2, where RS and AS stand for the retreating side and advancing side, respectively. It can be seen from the figure that the internal morphology of the AA1050-H24 weld is significantly different from that of the AA2017-T351 weld. In the AA1050-H24 weld, there is no weld nugget with elliptical rings no matter how much the welding parameters are changed, and there is not discernible interface between the stir zone and the TMAZ (Fig. 2(a)). In the AA2017-T351 weld, however, the weld nugget with "onion" rings clearly exists, and there is obvious plastic flow and a discernible interface between the nugget and the TMAZ

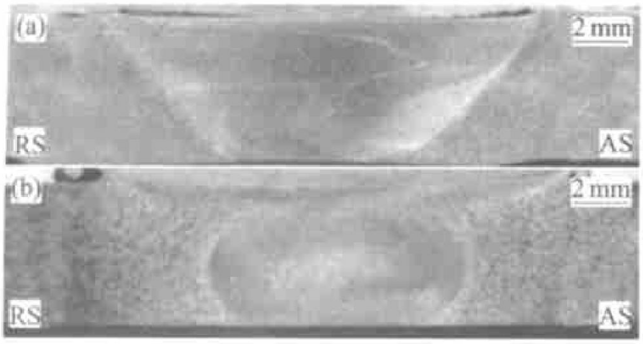

Fig. 2 Internal morphologies of AA1050-H24 welt at 0.07 mm•r^{-1}(a) and AA2017-T351 weld at 0.02 mm•r^{-1}(b)

(Fig. 2(b)).

In practice, the internal structures and morphologies of the defect-free welds have a decisive effect on the fracture paths of the joints. For example, the defect-free AA2017-T351 joint is fractured at or near the interface between the weld nugget and the TMAZ on the advancing side during the tensile test because a significant difference in the structure and morphology exists between the weld nugget and the TMAZ.

3.1.3 Internal defects of welds

Fig. 3 shows the internal defects of the AA1050-H24 and AA2017-T351 welds. It should be noted that these defects are formed at different revolutionary pitches. By comparing the defects shown in this figure, it can be found that the morphologies and distributions of the defects are different for the different aluminum alloys. The defect in the AA1050-H24 weld looks like a long crack, slightly sloping from the retreating side(RS) to the advancing side(AS), and is located in the lower part of the weld(Fig. 3(a)). The defect in the AA2017-T351 weld is composed of many voids and distributed in the middle part of the weld(Fig. 3(b)).

3.2 Mechanical properties and welding parameters

3.2.1 Mechanical properties of joints

For the sake of comparison, a designation called property efficiency is introduced in this paper. It is defined as the ratio of any property of a joint to the corresponding property of the base material. For example, the tensile strength efficiency of a joint is the ratio of the tensile strength of the joint to the tensile strength of the base material.

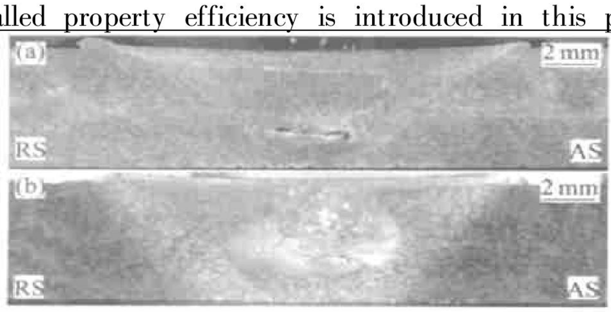

Fig. 3 Internal defects of AA1050-H24 weld at 0.40 mm•r^{-1}(a) and AA2017-T351 weld at 0.27 mm•r^{-1}(b)

Fig. 4 shows the mechanical property efficiencies of the AA1050-H24 and AA2017-T351 joints, including tensile strength efficiency (η_{TSE}) and elongation efficiency(η_{EE}). According to the figure, the property efficiencies of all the joints are lower than 100% except the maximum η_{EE} of the AA1050-H24 joints. This implies that the FSW results in a degradation of the mechanical properties for the two aluminum alloys.

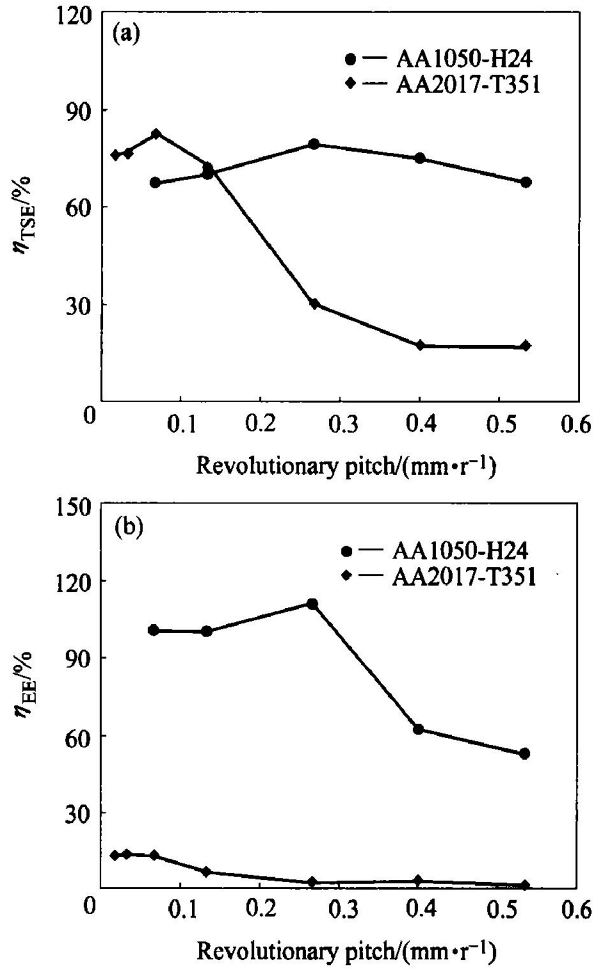

Fig. 4 Mechanical property efficiencies of joints for two aluminum alloys
(a) —η_{TSE}; (b) —η_{EE}

The maximum η_{TSE} of the AA1050-H24 and AA2017-T351 joints are 79% and 82%, respectively. This indicates that the tensile strengths of the aluminum alloys decrease at least by about 20% after the FSW.

The maximum η_{EE} values of the joints for the different aluminum alloys are significantly different from each other. They are 110% for AA1050-H24 and 14% for AA2017-T351. This indicates that the elongation of AA1050-H24 will not decrease if the optimum welding parameters are adopted during the FSW. However, the elongation of AA2017-T351 is seriously affected by the FSW.

3.2.2 Optimum welding parameters

As shown in Fig.4, the welding parameters have significant effects on the mechanical properties of the friction stir welded joints. Taking the comprehensive effects of the rotating speed and welding speed into account, we introduce a welding parameter called revolutionary pitch, and define a revolutionary pitch that can make the mechanical properties of the joint reach the highest as the optimum revolutionary pitch or optimum welding parameter.

Because of the difference in the physical, chemical and mechanical properties between the alloys, the optimum welding parameters for the different aluminum alloys are different from each other. With respect to AA1050-H24 and AA2017-T351 alloys, their optimum welding parameters are 0.27 $mm \cdot r^{-1}$ and 0.07 $mm \cdot r^{-1}$, respectively (Fig.4). In practice, when the real revolutionary pitch is greater than the optimum one, a welding defect occurs in the weld for lack of heat input to the joint (Fig.3), thus the joint is not qualified and accepted. Only when the real revolutionary pitch is smaller than or equal to the optimum one, can the mechanical properties of the joint be comparatively high. Therefore, the greater the optimum revolutionary pitch, the wider the selective or effective range of the welding parameters. From this point of view, it is easy to determine and understand that the effective ranges of welding parameters for AA1050-H24 and AA2017-T351 alloys are both narrow, especially for the latter. In other words, welding defects are easily formed in the AA1050-H24 and AA2017-T351 welds, especially in the latter.

4 CONCLUSIONS

1) The AA1050-H24 weld possesses a smooth surface and clear ripples, while the AA2017-T351 weld usually possesses a rough surface and visible ripples.

2) There is no elliptical weld nugget in the AA1050-H24 weld and there is not discernible interface between the stir zone and the TMAZ, while the elliptical weld nugget clearly exists in the AA2017-T351 weld and there is obvious plastic flow and a discernible interface between the nugget and the TMAZ.

3) The internal defect of the AA1050-H24 weld looks like a long crack and is located in the lower part of the weld, while that of the AA2017-T351 weld is composed of many voids and distributed in the middle part of the weld.

4) The effective ranges of the welding parameters for AA1050-H24 and AA2017-T351 are both narrow, especially for the latter.

5) The tensile strength efficiencies of the joints for the two typical alloys are similar to each other, ie 79% for AA1050-H24 and 82% for AA2017-T351.

REFERENCES

[1] Okamula H, Aota K, Ezumi M. Friction stir welding of aluminum alloy and application to structure[J]. J Jap Inst Light Met, 2000, 50: 166-171.

[2] Dawes C J, Thomas W M. Friction stir process welds aluminum alloys[J]. Weld J, 1996, 75: 41-45.

[3] Knipstrom K E, Pekkari B. Friction stir welding process goes commercial[J]. Weld J, 1997, 76: 55-57.

[4] Johnsen M R. Friction stir welding takes off at being[J]. Weld J, 1999, 78: 35-39.

[5] Campbell G, Stotler T. Friction stir welding of armor grade aluminum plate[J]. Weld J, 1999, 78: 45-47.

[6] Dawes M G, Karger S A, Dickerson T L, et al. Strength and fracture toughness of friction stir welds in aluminum alloys[A]. Proc 2nd Int Friction Stir Welding Symp[C]. Gothenburg, Sweden, TWI Ltd and IVF, 2000.

[7] Benavides S, Li Y, Murr L E, et al. Low-temperature friction stir welding of 2024 aluminum [J]. Scripta Mater, 1999, 41: 809-815.

[8] Hashimoto T, Jyogan S, Nakata K, et al. FSW joints of high strength aluminum alloy[A]. Proc 1st Int Friction Stir Welding Symp[C]. California, USA, 1999.

[9] Biallas G, Braun R, Donne C D, et al. Mechanical properties and corrosion behavior of friction stir welded 2024-T3[A]. Proc 1st Int Friction Stir Welding Symp[C]. California, USA, 1999.

[10] Strombeck A V, Santos J F D, Torster F, et al. Fracture toughness behavior of FSW joints on aluminum alloys[A]. Proc 1st Int Friction Stir Welding Symp[C]. California, USA, 1999.

[11] Kinchen D G, Li Z X, Adams G P. Mechanical properties of friction stir welds in Al-Li 2195-T8[A]. Proc 1st Int Friction Stir Welding Symp[C]. California, USA, 1999.

[12] Mahoney M W, Rhodes C G, Flintoff J G, et al. Properties of friction stir welded 7075-T651 aluminum[J]. Metall Mater Trans A, 1998, 29A: 1955-1964.

[13] Magnusson L, Kallman L. Mechanical properties of friction stir welds in thin sheet of aluminum 2024, 6013 and 7475[A]. Proc 2nd Int Friction Stir Welding Symp [C]. Gothenburg, Sweden, 2000.

[14] Jin H, Saimoto S, Ball M, et al. Characterization of microstructure and texture in friction stir welded joints of 5754 and 5182 aluminum alloy sheets[J]. Mater Sci Technol, 2001, 17: 1605-1614.

[15] Flores O V, Kennedy C, Murr L E, et al. Microstructural issues in a friction stir welded aluminum alloy[J]. Scripta Mater, 1998, 38: 703-708.

[16] Sato Y S, Urata M, Kokawa H, et al. Effect of friction stir processing on microstructure and hardness profile of equal channel angular pressed aluminum alloy 1050[A]. Proc 7th Int Friction Stir Welding Symp[C]. Kobe, Japan, 2001.

[17] Sato Y S, Urata M, Kokawa H, et al. Retention of the grained microstructure of equal channel angular pressed aluminum alloy 1050 by friction stir welding[J]. Scripta Mater, 2001, 45: 109-113.

(Edited by CHEN Wei-ping)